



OPEN ACCESS

EDITED BY

Vikash Kumar,
Central Inland Fisheries Research Institute
(ICAR), India

REVIEWED BY

Sofia Priyadarsani Das,
National Taiwan Ocean University, Taiwan
Soumya Prasad Panda,
Central Inland Fisheries Research Institute
(ICAR), India

*CORRESPONDENCE

Florybeth F. La Valle
✉ florybeth.lavalle@pepperdine.edu

RECEIVED 06 September 2023

ACCEPTED 03 November 2023

PUBLISHED 22 November 2023

CITATION

Jacobs JM, Himes L and La Valle FF (2023) *In situ* carbon uptake of marine macrophytes is highly variable among species, taxa, and morphology. *Front. Mar. Sci.* 10:1290054.
doi: 10.3389/fmars.2023.1290054

COPYRIGHT

© 2023 Jacobs, Himes and La Valle. This is an open-access article distributed under the terms of the [Creative Commons Attribution License \(CC BY\)](#). The use, distribution or reproduction in other forums is permitted, provided the original author(s) and the copyright owner(s) are credited and that the original publication in this journal is cited, in accordance with accepted academic practice. No use, distribution or reproduction is permitted which does not comply with these terms.

In situ carbon uptake of marine macrophytes is highly variable among species, taxa, and morphology

Julian M. Jacobs¹, Lucian Himes² and Florybeth F. La Valle^{2*}

¹Environmental Studies Program, Hamilton College, Clinton, NY, United States, ²Natural Science Division, Pepperdine University, Malibu, CA, United States

Macroalgae form important coastal ecosystems and are considered to be highly productive, yet individual macrophyte carbon uptake rates are poorly documented and methodologies for *in situ* assessments of productivity are not well developed. In this study, we employ a ^{13}C enrichment method in benthic chambers to calculate carbon uptake rates and assess $\delta^{13}\text{C}$ signatures of a large stock of nearshore benthic macroalgae varying in taxa and morphology in Southern California. Our objectives are to 1) identify the variability of carbon uptake and inorganic carbon use among individuals of the same species or morphology, and 2) establish accurate and accessible carbon uptake procedures for coastal benthic primary producers. We found no significant relationship between the observed ranges of environmental factors such as nutrient concentrations, PAR, temperature, conductivity, and productivity rates, suggesting that unique physiological complexities underpin the high variability of carbon uptake and $\delta^{13}\text{C}$ in studied macrophyte samples. We consider three reasons our experimental carbon uptake rates are 3–4 orders of magnitude lower than existing literature, which reports carbon uptake in the same units despite using different methods: 1) underrepresentation of P_{max} , 2) incomplete carbon fractionation corrections, and 3) reduced hydrodynamics within the benthic chambers.

KEYWORDS

carbon uptake₁, macroalgae₂, primary productivity₃, ^{13}C ₄, isotope enrichment₅, benthic chambers₆, *in situ*₇, marine algae₈

1 Introduction

Photosynthesis provides the primary source of organic matter in all aquatic ecosystems ([Falkowski and Raven, 2013](#); [Krause-Jensen et al., 2016](#)). As a result, the rate of photosynthesis places an upper limit on the biomass and productivity of ecosystems, making the study of primary productivity key to understanding the constraints of the biological flow of energy as well as the regulation of inorganic carbon and nutrient regimes and the greater global carbon cycle ([Falkowski and Raven, 2013](#)). Macroalgae are the

predominate primary producers on nearly one-third of global coastlines (Krause-Jensen et al., 2016; Queiros et al., 2023; Duarte et al., 2022), serve as a foundation species, and provide a variety of ecosystem services to local biota and humans (Pfister et al., 2019; Ruhamak et al., 2019; James et al., 2022). Studying the productivity of macroalgae is therefore essential to understanding the physical, chemical, and ecological functioning of nearshore marine environments, particularly under environmental shifts associated with climate change.

Benthic macroalgae assemblages rank among the most productive habitats on earth (Mann, 1973; Tait and Schiel, 2018), with a net primary productivity (NPP) up to ten times higher than that of temperate coastal phytoplankton (Pessarrodona et al., 2022) and comparable to that of tropical rainforests by area (Pace and Lovett, 2013; Duarte et al., 2022). Individual macrophyte productivity rates, however, are poorly defined (Dolliver and O'Connor, 2022), leading to uncertain carbon sequestration estimations and community biomass limits, and obscuring the effectiveness of algae aquaculture and ocean-based carbon dioxide removal (CDR) practices that employ macroalgae (Krause-Jensen et al., 2016).

Oxygen evolution and carbon assimilation measurements are the two most traditional methods of resolving the productivity of macrophytes (Peterson, 1980; Miller and Dunton, 2007; Pace and Lovett, 2013). In recent decades, the vast majority of macroalgae productivity assessments (Littler and Murray, 1974; Tait and Schiel, 2018; James et al., 2022) have employed the oxygen evolution technique, first described by Strickland (1960). The oxygen evolution technique uses the quantity of dissolved oxygen produced in light vs. dark incubations as a metric for NPP and community respiration (Littler and Murray, 1974; Mateo et al., 2001; Spector and Edwards, 2020).

The growing importance of climate-related research and applied carbon accounting, however, has encouraged calculating productivity in carbon units. This is inherently problematic for the oxygen evolution technique, and variable and often inconsistent conversion factors from oxygen evolved to carbon assimilated prohibit reliable translations of productivity (Arístegui et al., 1996; Cornwall and Hurd, 2019). This conversion relies on a photosynthetic quotient (PQ) which may vary depending on the physiological state and nutrient status of the alga (Miller and Dunton, 2007; Cornwall and Hurd, 2019). Additional uncertainties with the oxygen evolution method lie in the supposition that light and dark respiration is equivalent (Pace and Lovett, 2013) and that only a negligible quantity of energy is used by other concurrent metabolic processes such as nitrate and nitrite reduction (Miller and Dunton, 2007), producing potentially inaccurate representations of raw productivity (Peterson, 1980).

Our study uses the stable isotope ^{13}C (in the form of bicarbonate $\text{NaH}^{13}\text{CO}_3$) as a label for a fraction of photosynthetically incorporated carbon within macroalgae and a direct measurement of carbon uptake. Using ^{13}C enrichment to calculate carbon uptake is a measurement of gross primary productivity (GPP) when deployed on short (i.e., hours) time scales because of the time lag between when labeled carbon is acquired by macrophyte tissue and when it becomes accessible to

respiratory cycles (Miller and Dunton, 2007). Using ^{13}C in enrichments is preferred to other forms of labeled carbon, such as $^{14}\text{C}-\text{CO}_2$, because it avoids the environmental and procedural hazards associated with handling radioactive material (Miller and Dunton, 2007) and can be used in tandem with other isotope analyses such as ^{15}N (Mateo et al., 2001).

This study examines the carbon uptake rates of macroalgal species from all three major taxa (i.e., Rhodophyta, Phaeophyta, and Chlorophyta) and spans five functional groups (e.g., articulated corallines, filamentous, kelps and fucoids, fleshy branched, and tubular or sheet) with diverse morphological traits and physiological mechanisms. We pair carbon uptake measurements with assessments of macroalgal $\delta^{13}\text{C}$ signatures to identify the variability of carbon uptake and inorganic carbon use among individuals of the same species and morphology (Cornwall et al., 2015). Our use of field-based measurements complements the existing breadth of laboratory and culture-based experiments to directly evaluate the varying contribution of macroalgae species to coastal primary productivity. *In situ* procedures are difficult to execute due to the logistical difficulties of working in the marine environment (Raven et al., 2002) but are often favored because they more accurately reproduce environmental and physiological conditions than laboratory settings (Miller and Dunton, 2007; Carvalho et al., 2009b).

We hypothesize that macrophyte carbon uptake will vary according to morphology such that species with greater surface area to volume ratios will yield higher carbon uptake rates (form-function hypothesis). Additionally, we anticipate that species with high carbon uptake rates will have lower isotopic carbon discrimination in the carbon acquisition process and therefore greater $\delta^{13}\text{C}$ signatures (impartial carbon acquisition hypothesis). A concluding methodological comparison between our study and results from previous literature is designed to present the advantages of and considerations with using the ^{13}C method and establish accurate and accessible carbon uptake procedures for coastal benthic primary producers. To our knowledge, this study presents the first assessments of macroalgal productivity via a ^{13}C enrichment method *in situ* using benthic chambers on the Pacific Coast of North America. The results from this study can be applied to understand the potential responses of macrophyte productivity to changing ocean chemistry associated with climate change.

2 Materials and methods

2.1 Study site description and experimental design

This study was conducted at the Latigo Point intertidal zone located in Malibu, Southern California (Figure 1). Our specific study area is a 15 by 15 meter tide pool that forms at low tides (< 0 m) on a rugged rocky substrate. This region is dominated by vegetation, with 50% cover of macroalgae and 14% cover of seagrass. Diffuse, high salinity (~34 ppt), and high nutrient submarine groundwater discharge (SGD) containing an average (\pm standard deviation) of $33.75 \pm 18.89 \mu\text{mol L}^{-1} \text{NO}_3^-$, 1.65 ± 0.52

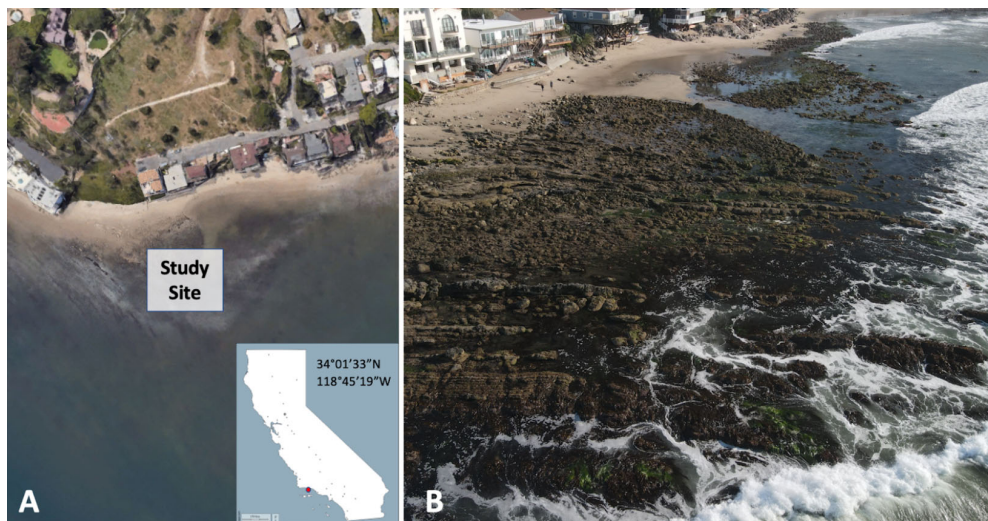


FIGURE 1
(A) Aerial view of the study site and inlaid map of study location in Southern California. **(B)** Photo of the intertidal zone at Latigo Point.

$\mu\text{mol L}^{-1}$ PO_4^{3-} , $33.1 \pm 8.15 \mu\text{mol L}^{-1}$ silicate, and $6.85 \pm 7.0 \mu\text{mol L}^{-1}$ NH_4^+ seeps from the sandy beach above as close as 25 meters from the study site. A small pipe 50 meters from the study area dispenses storm drainage runoff from nearby paved roads and residential housing complexes directly onto the beach. Latigo Canyon Creek, the principal tributary of the Latigo Canyon watershed, empties into the ocean 350 meters from the sampling site.

In situ benthic chambers are designed to isolate specimens and evaluate their response to manipulation in their natural setting and environmental conditions. Ten benthic chamber experiments were executed at low tides ranging from -0.02 meters to -0.3 meters at peak daylight hours (i.e., 9:00–14:00) from May to June. These methods closely follow those of [La Valle et al. \(2023\)](#) for benthic chambers. Benthic chambers were constructed from flexible clear six mil polyethylene bags (Polyethylene Greenhouse film, 93% PAR transparency) that allowed for movement of the chamber with water flow and had a sealable sampling port. Benthic chambers were placed around a rock containing a variety of macroalgal species and sealed to the hard substrate using multiple ring-shaped sandbags at the base with additional weighted chains placed on top of the sandbags. Each benthic chamber was designed to hold about 20 L of seawater and encompassed a 0.25 by 0.25 m area of benthos at its base. No air was permitted inside the benthic chamber after it was sealed to the benthos. Benthic chambers were then enriched with approximately 0.3 g of 98 at. % (atomic percent) $\text{NaH}^{13}\text{CO}_3$ at the start of the experiment and subsequently incubated for 1 hour.

Samples of macroalgae were picked from the specific location of the benthic chamber deployment site before sealing it to the substrate and after the hour-long incubation with $\text{NaH}^{13}\text{CO}_3$. To achieve an unbiased sampling protocol, specific species were not targeted in benthic chamber deployments; rather, suitable substrates with high macrophyte diversity were selected. Due to the diversity and spatial variability of macroalgae species at the study site, each benthic chamber contained a different array of species. All macroalgae were identified to the lowest possible

taxonomic level with the naked eye or scope in the laboratory after the experiment had concluded by cross-referencing morphology with identifications from established literature. Species that occurred more than once were included in data analysis performed in R.

2.2 Isotope analyses

Macroalgae samples were cleaned of sediments and epiphytes in the laboratory directly after the experiment and dried in aluminum tins at 60°C for 48–72 hours. Dried macrophyte tissue was ground in a Wig-L-Bug and packed in a standard-weight tin-pressed capsule according to methods described by [Teichberg et al. \(2008\)](#) and [de los Santos et al. \(2022\)](#). Samples were sent to the Center for Stable Isotope Biogeochemistry at the University of California at Berkeley to determine $\delta^{13}\text{C}$, $\delta^{15}\text{N}$, and total C and N by continuous flow (CF) dual isotope analysis using a CHNOS Elemental Analyzer interfaced to an IsoPrime100 mass spectrometer ([Carbon and Nitrogen Center for Stable Isotope Biogeochemistry](#)). Long-term external precision for C and N isotope determinations is $\pm 0.10\%$ and $\pm 0.20\%$, respectively.

2.3 Water chemistry and physical parameter measurements

Conductivity, temperature, and PAR: Salinity (Odyssey Temperature and Conductivity loggers, 3 to 60 mS cm^{-1}), temperature (Onset Tidbit v2 Water Temperature Data Logger), and photosynthetically active radiation (PAR) (Odyssey Submersible Photosynthetically Active Radiation logger) were monitored continuously at 1-minute intervals throughout the experiment. One set of sensors was placed within the benthic chamber and another set directly outside the benthic chamber in order to account for any environmental

differences influencing the study. [La Valle et al. \(2023\)](#) showed that this method does not significantly affect the PAR, temperature, and flow within the chamber compared to surrounding waters in coral reef systems.

Dissolved inorganic nutrients: Water samples for dissolved inorganic nutrient analysis were collected from the benthic chamber before the $\text{NaH}^{13}\text{CO}_3$ enrichment and after the hour-long experiment had concluded. Nutrient samples were also collected during the experiment from the local SGD, the storm drainage runoff, the Latigo Canyon Creek tributary, and 200 meters offshore. These samples were collected to quantify sources and ranges of nutrient concentrations at each location with respect to the study site. 60 mL water samples were filtered through $0.2\mu\text{M}$ glass fiber filters (Whatman), frozen at $< 0^\circ\text{C}$, and sent for analysis at Scripps Institute of Oceanography Shipboard Technical Support/Oceanographic Data Facility. Samples were thawed in a 50°C heating bath, brought to room temperature, and analyzed with a Seal Analytical continuous-flow AutoAnalyzer 3 (AA3). The final concentrations of nutrients were calculated using SEAL Analytical AACE software. Water samples were analyzed for soluble reactive phosphate (PO_4^{3-}) ammonium (NH_4^+), nitrate + nitrite ($\text{N} + \text{N}$; $\text{NO}_2^- + \text{NO}_3^-$), and silicate (SiO_4) using methods described by [Atlas et al. \(1971\)](#); [Hager et al. \(1972\)](#); [Gordon et al. \(1992\)](#), and [Becker et al. \(2019\)](#).

Dissolved inorganic carbon (DIC): 250 mL of water sample for DIC analysis was drawn from within the benthic chamber using a 500 mL syringe before the experiment, directly after the $\text{NaH}^{13}\text{CO}_3$ enrichment, and at the end of the hour-long incubation. DIC samples were stored in borosilicate bottles in dark-out bags and fixed with 20 μl HgCl_2 per 250 mL seawater within 2 hours of collection. Samples were sent to the Center for Stable Isotope Biogeochemistry at the University of California at Berkeley for $\delta^{13}\text{C}$ analysis according to procedures described by ([Torres et al., 2005](#)).

2.4 Numerical procedures and calculation of carbon uptake

Calculating carbon uptake requires defining the atomic % of ^{13}C within the sample, determined from the $^{13}\text{C}/^{12}\text{C}$ of the sample based on the deviation of $\delta^{13}\text{C}$ within the sample from the universal ^{13}C V-PDB (Vienna PeeDee Belemnite) standard designated by [Craig \(1957\)](#). All isotopic calculations are taken from [La Valle et al. \(2023\)](#) and [Hayes \(2004\)](#), outlined below, and described in detail in [Supplemental Table 1](#). Macroalgal carbon uptake rates were calculated using equation 1 below, derived from [Hama et al. \(1983\)](#) and used in [Mateo et al. \(2001\)](#) and [La Valle et al. \(2023\)](#). Similar calculations are also specified in [Cornelisen and Thomas \(2002\)](#).

$$\text{Macroalgae Carbon Uptake (mg C d}^{-1} \text{dw h}^{-1}) = \left(\frac{C \cdot (at_{enr} - at_{amb})}{t \cdot (at_{DIC} - at_{amb}) \cdot dw} \right) \cdot \alpha \quad (1)$$

Where at_{amb} is the atomic % ^{13}C in the ambient macrophyte tissue, at_{enr} is the atomic % ^{13}C of the macrophyte tissue 1 hour after enrichment, and at_{DIC} is the atomic % ^{13}C of DIC within the incubation directly after enrichment. C (mg) is the total carbon content of the sample, dw refers to the dry weight (g) of the sample after 48–72 hours of drying, and t (h) is the length of the experiment in hours. Alpha (α) refers to the fractionation coefficient and is described below. Phytoplankton uptake rates were determined using a carbon uptake rate equation similar to that found in [Hama et al. \(1983\)](#).

Phytoplankton Carbon Uptake ($\text{ug C L}^{-1} \text{h}^{-1}$)

$$= \frac{POC \cdot (at_{enr} - at_{amb})}{t \cdot (at_{DIC} - at_{amb})} \quad (2)$$

POC refers to the particulate organic carbon (ug C L^{-1}) in the incubated sample. To account for isotopic discrimination, a fractionation coefficient, α , is calculated on an individual alga basis based on the following equation by [Miller and Dunton \(2007\)](#) and applied directly to raw carbon uptake rates.

$$\text{Fractionation coefficient } (\alpha) = \left(\frac{\delta^{13}\text{C}_{DIC} - \delta^{13}\text{C}_{amb}}{1000 + \delta^{13}\text{C}_{amb}} \right) + 1 \quad (3)$$

Where $\delta^{13}\text{C}_{DIC}$ refers to the $\delta^{13}\text{C}$ of ambient DIC, and $\delta^{13}\text{C}_{amb}$ refers to the $\delta^{13}\text{C}$ of ambient macrophyte tissue.

3 Results

A total of 47 samples of macroalgae, spanning 12 species in all three major phyla, were collected and analyzed for carbon uptake rates and $\delta^{13}\text{C}$ signatures. Samples were partitioned into functional groups which were determined by organizing macrophytes based on surface area to volume ratios (SA:V) according to the categorizations of [Littler and Arnold \(1982\)](#), amended by [Murray and Bray \(1993\)](#), and are synonymous with algal morphological groups. The most common morphology is the tubular or sheet group, comprised of 13 samples across 4 species. All four tubular or sheet species in our study have a thin and flat quality. The next most common morphologies are the articulated corallines (2 species, $n = 9$), characterized by their CaCO_3 structure, the fleshy branched alga (2 species, $n = 9$) of feathery composition, and the kelps and fucoids (2 species, $n = 8$) with large branching fronds. Finally, the filamentous alga (2 species, $n = 7$) have distinct threadlike thalli.

[Figure 2](#) reveals that carbon uptake varied greatly on individual macrophyte and functional group scales. There were significant differences between species ($F_{11,34} = 2.846$, $p = 0.009$) and between functional groups ($F_{4, 41} = 6.493$, $p = 0.0004$) as indicated by a one-way ANOVA. Carbon uptake rates for sampled macroalgae ranged from an average of $2.05 \times 10^{-4} \text{ mgC g dry wt}^{-1} \text{ h}^{-1}$ (*J. macmillanii*) to $1.66 \times 10^{-3} \text{ mgC g dry wt}^{-1} \text{ h}^{-1}$ (*U. californica*). The articulated coralline functional group exhibited the lowest average carbon uptake among functional groups ($2.02 \times 10^{-4} \pm 1.47 \times 10^{-4} \text{ mgC g dry wt}^{-1} \text{ h}^{-1}$), followed by the filamentous group ($4.38 \times 10^{-4} \pm 2.28 \times 10^{-4} \text{ mgC g dry wt}^{-1} \text{ h}^{-1}$), the kelps and fucoids ($8.02 \times 10^{-4} \pm 6.71$

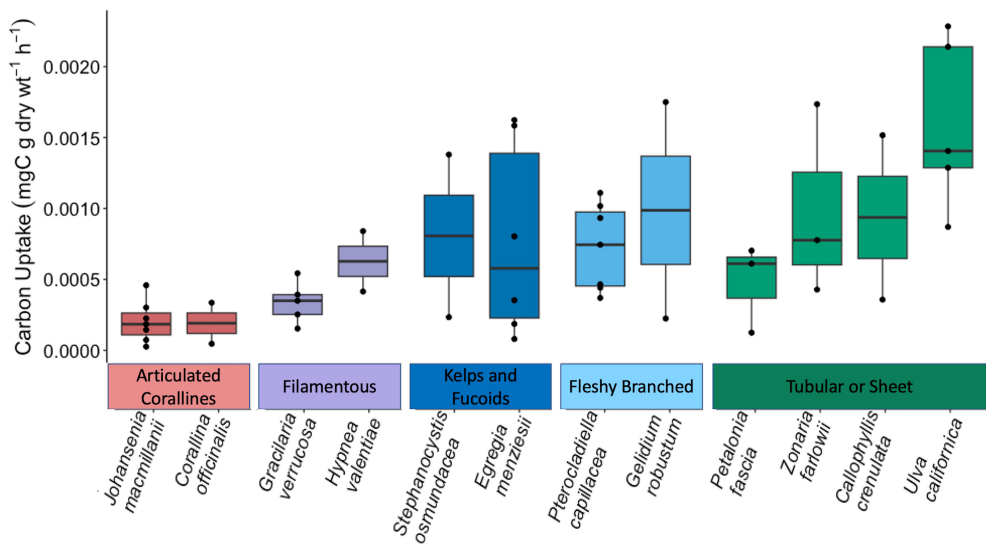


FIGURE 2

Boxplot displaying the carbon uptake rates of each macroalgae species. Species are displayed within their functional group from least productive (left) to most productive (right). Functional groups are also displayed from least productive (left: articulated corallines) to most productive (right: tubular or sheet).

$\times 10^{-4}$ mgC g dry wt $^{-1}$ h $^{-1}$), the fleshy branched group ($8.03 \times 10^{-4} \pm 4.85 \times 10^{-4}$ mgC g dry wt $^{-1}$ h $^{-1}$), and finally, the tubular or sheet group yielded the highest average carbon uptake ($1.13 \times 10^{-3} \pm 7.25 \times 10^{-4}$ mgC g dry wt $^{-1}$ h $^{-1}$). The homogeneity and normality of residuals prompted a log transformation of carbon uptake rates for statistical analysis. Tukey *post-hoc* analysis indicated significant differences between the articulated coralline group and the fleshy branched, tubular or sheet, and kelps and fucoids groups ($p = 0.0039$, $p = 0.0002$, $p = 0.034$ respectively). Significant differences were also found between species *J. macmillanii* and *U. californica* ($p = 0.0028$). Relationships between *C. officinalis* and *U. californica* and between *J. macmillanii* and *P. capillacea* approached significance ($p = 0.056$ and $p = 0.084$ respectively). In all cases, the alpha error rate was taken to be 5%. In terms of taxa, the Chlorophyta had the highest average carbon uptake rates ($1.66 \times 10^{-3} \pm 0.65 \times 10^{-3}$ mgC g dry wt $^{-1}$ h $^{-1}$), followed by the Phaeophyta ($7.77 \times 10^{-4} \pm 6.02 \times 10^{-4}$ mgC g dry wt $^{-1}$ h $^{-1}$), and finally the Rhodophyta ($5.2 \times 10^{-4} \pm 4.45 \times 10^{-4}$ mgC g dry wt $^{-1}$ h $^{-1}$).

$\delta^{13}\text{C}$ signatures ranged across all species from $-20.17\text{\textperthousand}$ (*C. crenulata*) to $-5.53\text{\textperthousand}$ (*J. macmillanii*). This also represents the range of $\delta^{13}\text{C}$ signatures of the Rhodophyta while the Chlorophyta $\delta^{13}\text{C}$ ranged from $-17.15\text{\textperthousand}$ to $-12.65\text{\textperthousand}$ and the Phaeophyta ranged from $-18.21\text{\textperthousand}$ to $-11.51\text{\textperthousand}$. A Kruskal-Wallis test with Dunn *post-hoc* analysis confirmed high variability of $\delta^{13}\text{C}$ and revealed significant differences between functional groups (Chi square = 17.2, $p = 0.002$, df = 4). The articulated corallines had the highest average $\delta^{13}\text{C}$ ($-9.90\text{\textperthousand} \pm 2.76\text{\textperthousand}$), followed by the fleshy branched group ($-13.61\text{\textperthousand} \pm 4.47\text{\textperthousand}$), the kelps and fucoids ($-15.35\text{\textperthousand} \pm 2.14\text{\textperthousand}$), the filamentous group ($-15.70\text{\textperthousand} \pm 2.58\text{\textperthousand}$), and finally the tubular or sheet group ($-16.03\text{\textperthousand} \pm 2.50\text{\textperthousand}$). The articulated coralline functional group was determined to be significantly different in $\delta^{13}\text{C}$ compared to the tubular or sheet, kelps and fucoids, and filamentous groups ($p = 0.001$, $p = 0.026$, $p = 0.026$ respectively).

The Kruskal-Wallis test with Dunn *post-hoc* analysis also revealed significant differences between species (Chi squared = 29.98, $p = 0.002$, df = 11) such that *J. macmillanii* was significantly greater in $\delta^{13}\text{C}$ compared to *C. crenulata*, *E. menziesii*, and *H. valentiae* ($p = 0.016$, $p = 0.031$, $p = 0.04$ respectively) and *Z. farlowii* was significantly lower in $\delta^{13}\text{C}$ than *P. capillacea* ($p = 0.04$). A complete list $\delta^{13}\text{C}$ values from all 12 species and 5 functional groups is provided in Table 1.

We compared our carbon uptake rates to those of Littler and Arnold (1982) because of their integral work in establishing productivity measurements for marine macrophytes and because of the use of different methodologies to achieve productivity rates with the same units (mg C g dry wt $^{-1}$ h $^{-1}$). In contrast with our methods, Littler and Arnold (1982) incubated individual macrophytes away from the benthos and observed oxygen evolution in light and dark bottles according to methods first described by Littler and Murray (1974). The quantity of produced oxygen was then converted to carbon uptake to estimate NPP via a photosynthetic quotient which was assumed to be a constant PQ = 1 (Littler and Arnold, 1982). Experimental carbon uptake rates are 3–4 orders of magnitude lower than those of Littler and Arnold (1982). Comparative data is listed in Table 2. The comparison between these methodologies is important because they represent the two most fundamental ways to measure primary productivity.

4 Discussion

4.1 Carbon uptake rates and the form-function hypothesis

To our knowledge, this is the first study to calculate carbon uptake rates of macroalgae *in situ* using a ^{13}C enrichment method in

TABLE 1 Species-specific carbon uptake rates and ambient $\delta^{13}\text{C}$ values of macrophyte tissue, including phytoplankton within the benthic chamber.

Functional Group	Species	Average carbon uptake (mg C g dry wt $^{-1}$ h $^{-1}$) \pm standard deviation	Average $\delta^{13}\text{C}$ of ambient macroalgal tissue (‰) \pm standard deviation
Articulated Corallines	<i>Johansenia macmillanii</i>	$2.05 \times 10^{-4} \pm 1.47 \times 10^{-4}$ n = 7	-9.17 \pm 2.18 n = 7
	<i>Corallina officinalis</i>	$1.95 \times 10^{-4} \pm 2.08 \times 10^{-4}$ n = 2	-12.83 \pm 3.71 n = 2
Filamentous	<i>Gracilaria verrucosa</i>	$3.50 \times 10^{-4} \pm 1.53 \times 10^{-4}$ n = 5	-14.51 \pm 1.93 n = 5
	<i>Hypnea valentiae</i>	$6.58 \times 10^{-4} \pm 2.89 \times 10^{-4}$ n = 2	-18.66 \pm 0.66 n = 2
Kelps and Fucoids	<i>Stephanocystis osmundacea</i>	$8.22 \times 10^{-4} \pm 8.22 \times 10^{-4}$ n = 2	-12.4 \pm 1.26 n = 2
	<i>Egregia menziesii</i>	$7.96 \times 10^{-4} \pm 7.03 \times 10^{-4}$ n = 6	-16.19 \pm 1.45 n = 6
Fleshy Branched	<i>Pterocladiella capillacea</i>	$7.46 \times 10^{-4} \pm 3.09 \times 10^{-4}$ n = 7	-14.24 \pm 3.98 n = 7
	<i>Gelidium robustum</i>	$1.00 \times 10^{-3} \pm 1.10 \times 10^{-3}$ n = 2	-11.42 \pm 7.25 n = 2
Tubular or Sheet	<i>Petalonia fascia</i>	$4.87 \times 10^{-4} \pm 3.16 \times 10^{-4}$ n = 3	-14.92 \pm 2.66 n = 3
	<i>Zonaria farlowii</i>	$1.00 \times 10^{-3} \pm 6.87 \times 10^{-4}$ n = 3	-17.15 \pm 1.17 n = 3
	<i>Callophyllis crenulata</i>	$9.62 \times 10^{-4} \pm 8.39 \times 10^{-4}$ n = 2	-20.04 \pm 0.18 n = 2
	<i>Ulva californica</i>	$1.66 \times 10^{-3} \pm 6.55 \times 10^{-4}$ n = 5	-14.69 \pm 1.69 n = 5
Phytoplankton	Unknown	$1.44 \times 10^{-1} \pm 1.52 \times 10^{-1}$ (mgC L $^{-1}$ h $^{-1}$) n = 6	-20.80 \pm 3.07 n = 6

benthic chambers on the Pacific Coast of North America. Our study reveals carbon uptake rates vary among functional groups such that articulated corallines have the lowest average productivity rates and tubular or sheet forms have the highest, differing significantly ($p = 0.0002$) (Figure 2). This supports the form and function hypothesis developed by Littler and Arnold (1982), describing the physiological tradeoffs between surface area (SA) and volume (V) as it relates to

TABLE 2 Ambient $\delta^{13}\text{C}$ signatures and carbon uptake rates for each functional group from experimental data and Littler and Arnold (1982).

Functional Group	$\delta^{13}\text{C}$ of ambient macroalgal tissue (‰) \pm standard deviation	Average carbon uptake (mgC g dry wt $^{-1}$ h $^{-1}$) \pm standard deviation (Experimental data)	Carbon uptake (mgC g dry wt $^{-1}$ h $^{-1}$) \pm standard deviation (Littler and Arnold (1982). Modified by Murray and Bray (1993))
Articulated Corallines	-9.9 \pm 2.76 n = 9	$2.02 \times 10^{-4} \pm 1.47 \times 10^{-4}$ n = 9	0.7 \pm 0.6 n = 15
Filamentous	-15.70 \pm 2.58 n = 7	$4.38 \times 10^{-4} \pm 2.28 \times 10^{-4}$ n = 7	2.0 \pm 1.8 n = 8
Kelps and Fucoids	-15.35 \pm 2.14 n = 8	$8.02 \times 10^{-4} \pm 6.71 \times 10^{-4}$ n = 8	1.3 \pm 0.9 n = 26
Fleshy Branched	-13.61 \pm 4.47 n = 9	$8.03 \times 10^{-4} \pm 4.85 \times 10^{-4}$ n = 9	1.5 \pm 0.8 n = 27
Tubular or Sheet	-16.03 \pm 2.50 n = 14	$1.13 \times 10^{-3} \pm 7.25 \times 10^{-4}$ n = 14	5.0 \pm 2.6 n = 17

the distribution of energy between structural development and photosynthetic production. Stewart and Carpenter (2003) agree that growth strategies designed to limit damage to the thallus are a principal driver of morphological plasticity in macrophytes and might directly reduce their ability to reach maximum photosynthetic capacity. Considering this tradeoff, we can attribute the lowest uptake rates of the articulated corallines to a prioritization of building robust geometrically complex and calcified structures (Littler and Littler, 1981; Williamson et al., 2017; Ryznar et al., 2021), and the high uptake rates of the tubular or sheet forms to high SA:V ratios which imply an emphasis on photosynthetic productivity (Tsubaki et al., 2020).

The three other functional groups identified in our study (i.e., filamentous, kelps and fucoids, and fleshy branched) have carbon uptake rates between the previously mentioned classifications, are not statistically different, and do not directly follow the form-function hypothesis (Figure 3). While the form-function hypothesis based on SA:V ratios explains the extremes of macroalgae productivity in our samples, the comparative productivity of macrophytes cannot solely be predicted by morphology. Additionally, carbon uptake rates do not show significant relationships with environmental factors including ambient nutrient concentrations, PAR, conductivity, temperature, and DIC (Supplementary Table 2, Supplementary Table 3). The lack of correlations between observed ranges of exterior environmental

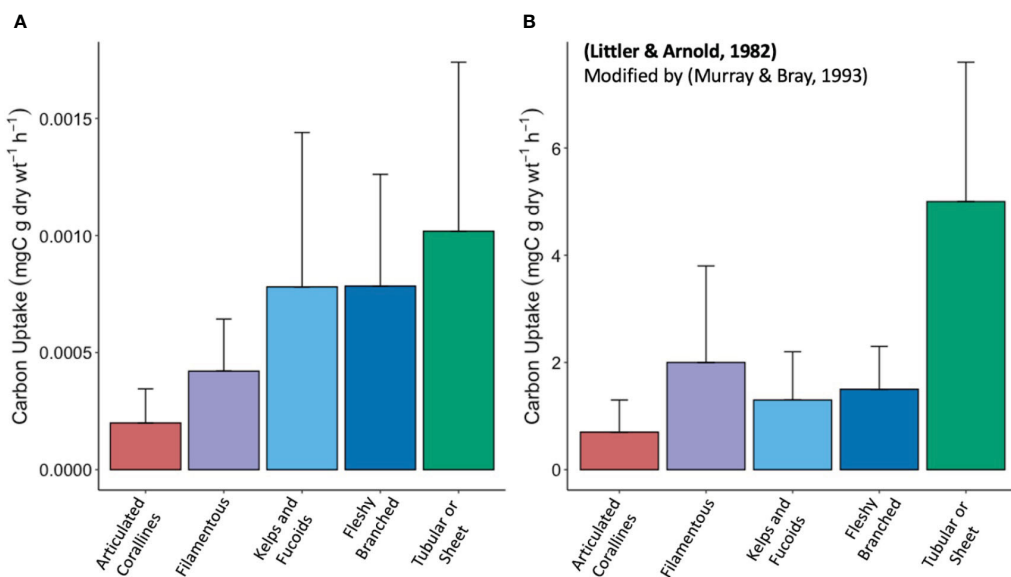


FIGURE 3

(A) Barplot of carbon uptake rates of functional groups from experimental data including standard deviations (B) Barplot of carbon uptake rates of functional groups from Littler and Arnold (1982) including standard deviations. Number of samples for each functional group in (A), experimental data, is articulated corallines ($n = 9$), filamentous ($n = 7$), kelps and fucoids ($n = 8$), fleshy branched ($n = 9$), and tubular or sheet ($n = 13$). The number of samples for each functional group in panel B, from Littler and Arnold (1982), is articulated corallines ($n = 15$), filamentous ($n = 8$), kelps and fucoids ($n = 26$), fleshy branched ($n = 27$), and tubular or sheet ($n = 17$). Different sample sizes between the studies are a result of our selection of study sites with random macrophyte diversity.

factors and carbon uptake position individual macrophyte physiology at the core of the variability in carbon uptake in our study. As a result, we caution against making general estimations of community-level productivity based on the productivity rates of individuals.

4.2 $\delta^{13}\text{C}$ and implications for carbon acquisition strategies

Bicarbonate is the preferred medium to introduce labeled DIC (^{13}C) and directly measure carbon uptake for marine macrophytes due to its natural abundance in marine ecosystems and the high concentration of carbon concentrating mechanisms (CCMs) in macroalgae (Cornwall et al., 2015; Zweng et al. 2018). While the passive diffusion of CO_2 into tissue is the least energetically expensive route of carbon acquisition for macrophytes (Cornwall et al. 2012; Diaz-Pulido et al., 2016), CO_2 only accounts for 1% ($\sim 10\text{--}20 \mu\text{M}$) of seawater DIC (James et al., 2022; Capó-Bauzá et al., 2023) and diffuses into photosynthetic tissue 10,000 times slower in water than in air (Bergstrom et al., 2020; Capó-Bauzá et al., 2023). This has prompted the selection of CCMs in macroalgae that exploit the more abundant bicarbonate, accounting for 92% - 98% of seawater DIC ($\sim 1700\text{--}2100 \mu\text{M}$) (Rautenberger et al., 2015; James et al., 2022) by converting HCO_3^- to CO_2 intracellularly at the site of Rubisco where it is fixed for photosynthesis (Raven et al., 1995; Miller and Dunton, 2007; Ji and Gao, 2021).

Since macroalgae utilize the lighter and more abundant ^{12}C quicker than ^{13}C as a result of fractionation during carbon

assimilation, the carbon uptake mechanism (i.e., CCM or non-CCM) of an individual macrophyte can be inferred from its $\delta^{13}\text{C}$ signature (Lovelock et al., 2020; Velázquez-Ochoa et al., 2022). This is because each species of DIC in seawater has a specific affinity for ^{13}C with CO_2 , HCO_3^- , and CO_3^{2-} having average $\delta^{13}\text{C}$ signatures of -10‰ , -0.5‰ , and 2‰ , respectively (Kroopnick, 1985; Velázquez-Ochoa et al., 2022). Accordingly, species that employ CCMs are expected to have proportionally higher $\delta^{13}\text{C}$ values within their tissue than their non-CCM counterparts (Raven et al., 2002).

Macrophytes can be categorized into three approximate strategies according to their use of CCMs: (1) entirely active HCO_3^- diffusion ($\delta^{13}\text{C} > -10 \text{‰}$), (2) utilizing both passive CO_2 and active HCO_3^- diffusion ($-10 \text{‰} > \delta^{13}\text{C} > -30 \text{‰}$), and (3) exclusive diffusive entry of CO_2 ($\delta^{13}\text{C} < -30 \text{‰}$) (Cornwall et al., 2015; Diaz-Pulido et al., 2016; Velázquez-Ochoa et al., 2022). Macroalgae samples in the present study show high $\delta^{13}\text{C}$ variability across taxa and morphological groups. All macroalgae in this study have a $\delta^{13}\text{C} > -30 \text{‰}$ (Table 1), indicating that their carbon requirements are satisfied, either partially or fully, by bicarbonate (Raven et al., 2002; Giordano et al., 2005; Hepburn et al., 2011). The majority of our samples (86%) utilize varying degrees of HCO_3^- and CO_2 , and only 14% of our total samples have $\delta^{13}\text{C} > -10 \text{‰}$ and solely rely on bicarbonate during carbon acquisition (Figure 4).

The Rhodophyta have the greatest range of $\delta^{13}\text{C}$ values (-20.17‰ to -5.53‰), suggesting the use of a diverse array of carbon uptake strategies. The articulated coralline functional group, belonging exclusively to the Rhodophyta, has the highest average $\delta^{13}\text{C}$ ($-9.9 \text{‰} \pm 2.76 \text{‰}$), significantly lower than the tubular or

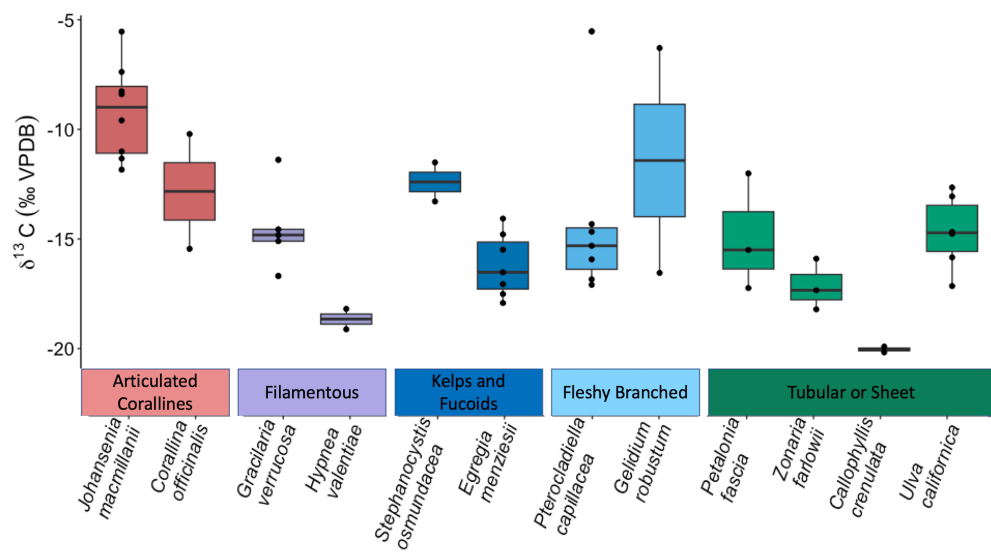


FIGURE 4

Boxplot displaying $\delta^{13}\text{C}$ in ambient macrophyte tissue across species and among functional groups. Species are not ranked by $\delta^{13}\text{C}$ signature, rather the display order follows the ranking of the carbon uptake rates as described in the [Figure 2](#) caption.

sheet, kelps and fucoids, and filamentous groups ($p = 0.001$, $p = 0.026$, $p = 0.026$ respectively) ([Table 2](#)), implying a preference for bicarbonate ([Carvalho et al., 2009b](#)). This can be explained by the integral role of bicarbonate assimilation in meeting the high energetic requirements of calcification via chemical buffering to low pH ([Hepburn et al., 2011](#); [Cornwall et al., 2017](#)). Therefore, bicarbonate assimilation for the articulated corallines serves the dual function as a substrate for photosynthesis and maintenance of complex and energetically expensive morphology.

Species with high photosynthetic activity have high carbon requirements and it has been proposed that these species have lower isotopic carbon discrimination ([Carvalho et al., 2010](#); [Rautenberger et al., 2015](#); [Velázquez-Ochoa et al., 2022](#)). This is not the case in our results and contradicts our impartial carbon acquisition hypothesis as highly productive species such as *U. californica* and *C. crenulata* have among the highest discrimination values, and the articulated coralline species with low carbon uptake rates discriminate the least against ^{13}C . Strong variation of macrophyte $\delta^{13}\text{C}$ signatures among macrophytes of the same species implies a range of inorganic carbon use. This makes it difficult to quantify how macrophytes of a specific species will tolerate and perform under different ambient inorganic carbon regimes. As a result, more information than solely the degree of inorganic carbon species use is required to make general predictions about fitness in anticipated future ocean chemistries associated with climate change ([van der Loos et al. 2018](#)).

4.3 Considerations for variability in carbon uptake rates

Considerable variation is evident in both carbon uptake rates and $\delta^{13}\text{C}$ for macroalgae and it is important to consider the reality of such “snapshot” ([Raven et al., 1995](#)) measurements, representing

the algal physiology and the seawater chemistry at a specific point in time. *E. menziesii*, for example, has a small range of $\delta^{13}\text{C}$ values (-17.92 ‰ to -14.07 ‰) but the greatest range of any species in carbon uptake rates (8.17×10^{-5} to 1.65×10^{-3} $\text{mgC g dry wt}^{-1} \text{ h}^{-1}$), supporting that individuals of the same species and carbon complexion can express very different carbon uptake rates, likely resulting from unique physiological complexities. Varying anatomical location (e.g., thallus or holdfast), sample age, morphology, surrounding community structure, nutrient regimes, light acclimation, and desiccation ([Raven et al., 1995](#); [Lovelock et al., 2020](#); [Velázquez-Ochoa et al., 2022](#)) can all impact the photosynthetic performance and chemical composition of an alga. Additional sources of variability in carbon uptake among macrophytes can arise from seasonal variability ([Raven et al., 1995](#)), daily periodicity effects on production ([Littler and Murray, 1974](#)), and the geographic range from which the specimen originates ([Maberly et al., 1992](#)), but these factors are unlikely contributing to discrepancies within our data due to concentrated sampling protocols by location and time. It does, however, mean that these productivity rates may not be representative of other specimens collected at different locations or during a different season.

The most pronounced difference between experimentally derived carbon uptake rates and those of [Littler and Arnold \(1982\)](#), is that our experimental values are 3–4 orders of magnitude lower. Low experimental carbon uptake does not reflect the productivity rates of highly productive vegetation which we expected of our specimens of macroalgae. These comparatively low values, however, are most likely a result of discrepancies between data gathered with the oxygen evolution method and the ^{13}C enrichment method. The remainder of this discussion will be dedicated to exploring how our experimental procedures using ^{13}C may have resulted in an underestimation of carbon uptake rates. We theorize three potential reasons for this

underestimation: 1) underrepresentation of maximum photosynthetic rates, 2) incomplete consideration of fractionation in calculations, and 3) reduced water flow within the incubations.

4.3.1 Underrepresentation of maximum photosynthetic rates

Firstly, implicit in methods of *in situ* sampling is the underrepresentation of the absolute maximum photosynthetic rate (P_{\max}). [Miller and Dunton \(2007\)](#), using similar ^{13}C assimilation methods, estimated their experimental carbon uptake rate to be $<10\%$ P_{\max} with media at. % ^{13}C to be $>50\%$ in 1.5-hour incubations, showing that there are potentially high disparities between experimental and actual carbon uptake rates despite considerable introduction of ^{13}C . Comparatively, in our 1-hour incubation, at. % ^{13}C never reached above 20%, providing a possible explanation for low carbon uptake rates. Additionally, [Mateo et al. \(2001\)](#) found that an increase of seawater $\delta^{13}\text{C}$ of 34‰ is needed to achieve a 1% change in carbon uptake rates. These suggest that a substantial increase in DIC is required to induce measurable changes in at. % ^{13}C of macroalgae tissue. This is a potential drawback of using the ^{13}C enrichment method ([Miller and Dunton, 2007](#)).

4.3.2 Degrees of fractionation

Another fundamental consideration of using isotopes in biological systems is fractionation; in this case, the kinetic fractionation in carbon assimilation of the carbonic-anhydrase-catalyzed conversion of HCO_3^- to CO_2 in macroalgae ([Raven et al., 1995](#)). The average fractionation correction (α), based on the equation by [Miller and Dunton \(2007\)](#) and described in methods, of our macroalgae samples is 1.027 ± 0.02 and agrees with the widely used average from [Hama et al. \(1983\)](#) of 1.025, referring to discrimination in phytoplankton. There are two matters, however, that this fractionation correction equation does not account for that are potentially significant drivers of ^{13}C assimilation in algal tissue being the significant change in seawater chemistry after ^{13}C enrichment, and the high variability of ambient seawater $\delta^{13}\text{C}$ at our study site.

The fractionation coefficient is highly sensitive to the $\delta^{13}\text{C}$ of ambient seawater such that an increase of 50‰ $\delta^{13}\text{C}$ will increase the fractionation correction by a near-equal percentage (49%). This can be problematic because the fractionation coefficient is based on ambient $\delta^{13}\text{C}$ and the seawater medium $\delta^{13}\text{C}$ within our incubations changes dramatically after ^{13}C enrichment. The fractionation coefficient, a snapshot estimation of algal physiology before the experiment, might not represent the carbon assimilation strategies employed under different regimes of $\delta^{13}\text{C}$ which vary significantly throughout the incubation period.

This variability in fractionation is supported by highly variable ambient seawater $\delta^{13}\text{C}$ at our site. $\delta^{13}\text{C}$ has deviated from the reasonably uniform global seawater average of 1.07‰ ([Kroopnick, 1985](#); [Tsubaki et al., 2020](#)) such that our site has an average $\delta^{13}\text{C}$ (\pm standard deviation) of $2.42\% \pm 2.45\%$, and on consecutive days we have sampled values from 0.69‰ to 4.93‰, supporting that not only in our incubations but on a day-to-day basis, macrophytes at our study site are exposed to highly variable $\delta^{13}\text{C}$. It is possible that

this frequent variation has resulted in the development of malleable carbon acquisition mechanisms that are not implicit in the snapshot fractionation coefficient calculation. This discrimination plasticity has been explored by others including [Young and Beardall \(2005\)](#); [Carvalho et al. \(2009a\)](#); [Carvalho et al. \(2009b\)](#); [Carvalho et al. \(2010\)](#), and [Bergstrom et al. \(2020\)](#) but existing research to support carbon fractionation variation on such short temporal scales is presently absent.

4.3.3 Hydrodynamics

Two factors indicate that slow tracer diffusion is another potential influence on calculated carbon uptake rates. Back-calculations of benthic chamber volume and estimations of the percent by which we enriched our incubations can be inconsistent based on post-enrichment DIC concentrations. This suggests that at the time of post-enrichment DIC sampling, our introduced carbon could be poorly mixed, the post-enrichment DIC sample could be an underrepresentation of total carbon introduced, and our carbon uptake rates calculated with this value could be a misrepresentation of actual carbon uptake in our experiments ([Yacobi et al., 2007](#)). This highlights the importance of hydrodynamics for mixing the incubation media in benthic chambers ([Thomas and Cornelisen, 2003](#); [La Valle et al., 2019](#)).

Hydrodynamics is also integral for the exchange of assimilated and respired compounds to and from the macrophyte tissue ([Houlihan et al., 2020](#)). The interaction between the biological activity of the macrophyte and the surrounding seawater produces a diffusive boundary layer (DBL) at the algal-seawater interface ([Cornwall et al., 2013](#)), ranging from μm to cm thick ([Houlihan et al., 2020](#)), that is chemically unique from the surrounding seawater. DBLs can prevent the assimilation of inorganic carbon and nutrients under stagnant flow conditions ([Hurd, 2000](#); [Cornwall et al., 2015](#); [James et al., 2022](#)). Algal morphology and surrounding water velocity determine the thickness and influence of the DBL ([Raven and Hurd, 2012](#)) and therefore affect photosynthetic rates ([James et al., 2022](#)). If slow tracer diffusion is present within the incubations, it is likely that reduced hydrodynamics within our benthic chambers play a role in limiting carbon uptake and underestimating true photosynthetic rates.

In summary, this study is an important step toward better understanding the carbon uptake of macrophytes by using novel *in situ* procedures of ^{13}C enrichments. The lack of correlation between observed ranges of environmental factors and carbon uptake suggests that unique macrophyte physiologies underpin the high variability of productivity rates and $\delta^{13}\text{C}$ signatures in our study. As such, assumptions about macrophyte productivity and responses of macroalgae to changing ocean chemistry regimes cannot be generalized and require the acknowledgment of complex differences among individuals of the same species and origin. Repetition of *in situ* productivity assessments is needed to better comprehend the contribution of individual macrophytes to community-level primary productivity and to monitor changes in productivity associated with shifting ocean chemistry.

We suggest future research using the ^{13}C enrichment method to address the potential reasons for underestimation of carbon uptake, answering key remaining questions such as, does carbon

fractionation exhibit plasticity on short time scales in macrophytes? Does the physiology responsible for carbon uptake change at different saturations of carbon in seawater? Subsequent iterations of field-based benthic chambers are strongly encouraged with the underlying considerations of hydrodynamics and an emphasis on properly mixing introduced material. These field-based measurements are essential contributions to phycology research by providing direct estimations of carbon-based productivity rates.

Data availability statement

The datasets presented in this study can be found in online repositories. The names of the repository/repositories and accession number(s) can be found below: Our data and metadata was submitted to Pepperdine Digital Commons and will be submitted to the US National Science Foundation Biological and Chemical Oceanography Data Management Office (BCO-DMO) repository. Data is publicly available at the following link: <https://digitalcommons.pepperdine.edu/surb/29>

Author contributions

JJ: Conceptualization, Data curation, Formal Analysis, Investigation, Methodology, Visualization, Writing – original draft, Writing – review and editing. LH: Conceptualization, Data curation, Investigation, Methodology, Writing – review and editing. FL: Conceptualization, Funding acquisition, Methodology, Resources, Supervision, Writing – review and editing.

Funding

The author(s) declare financial support was received for the research, authorship, and/or publication of this article. This project

was funded by the Boyajian Fund, NSF DBI 1950350, NSF DEB 2312723, and Pepperdine University's Seaver Dean's Office and Division of Natural Sciences.

Acknowledgments

This project was funded by the Boyajian Fund, NSF DBI 1950350, NSF DEB 2312723, and Pepperdine University's Seaver Dean's Office and Division of Natural Sciences. Field and lab support was provided by S. Zummo, M. Sprute, C. Dao, J. Fuqua, R. Ang, J. Moser, M. Sadecki, H. Vaidya.

Conflict of interest

The authors declare that the research was conducted in the absence of any commercial or financial relationships that could be construed as a potential conflict of interest.

Publisher's note

All claims expressed in this article are solely those of the authors and do not necessarily represent those of their affiliated organizations, or those of the publisher, the editors and the reviewers. Any product that may be evaluated in this article, or claim that may be made by its manufacturer, is not guaranteed or endorsed by the publisher.

Supplementary material

The Supplementary Material for this article can be found online at: <https://www.frontiersin.org/articles/10.3389/fmars.2023.1290054/full#supplementary-material>

References

Aristegui, J., Montero, M., Ballesteros, S., Basterretxea, G., and Van Lenning, K. (1996). Planktonic primary production and microbial respiration measured by ^{14}C assimilation and dissolved oxygen changes in coastal waters of the Antarctic Peninsula during austral summer: implications for carbon flux studies. *Mar. Ecol. Prog. Ser.* 132, 191–201. doi: 10.3354/meps132191

Atlas, E. L., Hager, S. W., Gordon, L. I., and Park, P. K. (1971). *A Practical Manual for Use of the Technicon AutoAnalyzer in Seawater Nutrient Analyses Revised*. Technical Report. 215 (Oregon State University, Department of Oceanography), 71–22.

Becker, S., Aoyama, M., Woodward, E. M. S., Bakker, K., Coverly, S., Mahaffey, C., et al. (2019). “The precise and accurate determination of dissolved inorganic nutrients in seawater: Continuous Flow Analysis methods and laboratory practices,” in *IOC Report No. 14. GO-SHIP Repeat Hydrography Manual: A Collection of Expert Reports and Guidelines* (IOPC Publication Series No. 134).

Bergstrom, E., Ordoñez, A., Ho, M., Hurd, C., Fry, B., and Diaz-Pulido, G. (2020). Inorganic carbon uptake strategies in coralline algae: Plasticity across evolutionary lineages under ocean acidification and warming. *Mar. Environ. Res.* 161, 105107. doi: 10.1016/j.marenvres.2020.105107

Capó-Bauçà, S., Galmés, J., Aguiló-Nicolau, P., Ramis-Pozuelo, S., and Iñiguez, C. (2023). Carbon assimilation in upper subtidal macroalgae is determined by an inverse correlation between Rubisco carboxylation efficiency and CO_2 concentrating mechanism effectiveness. *New Phytol.* 237, 2027–2038. doi: 10.1111/nph.18623

Carbon and Nitrogen Center for Stable Isotope Biogeochemistry. Available at: <https://nature.berkeley.edu/stableisotopelab/analyses/organic-analysis/13c-15n-organic-analysis/> (Accessed June 21, 2023).

Carvalho, M. C., Hayashizaki, K., and Ogawa, H. (2009a). Carbon stable isotope discrimination: a possible growth index for the kelp *Undaria pinnatifida*. *Mar. Ecol. Prog. Ser.* 381, 71–82. doi: 10.3354/meps07948

Carvalho, M. C., Hayashizaki, K.-I., and Ogawa, H. (2009b). Short-term measurement of carbon stable isotope discrimination in photosynthesis and respiration by Aquatic macrophytes, with marine macroalgal examples. *J. Phycol.* 45, 761–770. doi: 10.1111/j.1529-8817.2009.00685.x

Carvalho, M. C., Hayashizaki, K., and Ogawa, H. (2010). Temperature effect on carbon isotopic discrimination by *Undaria pinnatifida* (phaeophyta) in a closed experimental system. *J. Phycol.* 46, 1180–1186. doi: 10.1111/j.1529-8817.2010.00895.x

Cornelisen, C. D., and Thomas, F. I. M. (2002). Ammonium uptake by seagrass epiphytes: Isolation of the effects of water velocity using an isotope label. *Limnol. Oceanogr.* 47, 1223–1229. doi: 10.4319/lo.2002.47.4.1223

Cornwall, C. E., Hepburn, C. D., Pilditch, C. A., and Hurd, C. L. (2013). Concentration boundary layers around complex assemblages of macroalgae: Implications for the effects of ocean acidification on understory coralline algae. *Limnol. Oceanogr.* 58, 121–130. doi: 10.4319/lo.2013.58.1.0121

Cornwall, Hepburn, and Pritchard, (2012). CARBON-USE STRATEGIES IN MACROALGAE: DIFFERENTIAL RESPONSES TO LOWERED PH AND IMPLICATIONS FOR OCEAN ACIDIFICATION. *J. Phycol.* 48, 137–144. doi: 10.1111/j.1529-8817.2011.01085.x

Cornwall, C. E., and Hurd, C. L. (2019). Variability in the benefits of ocean acidification to photosynthetic rates of macroalgae without CO₂-concentrating mechanisms. *Mar. Freshw. Res.* 71, 275–280. doi: 10.1071/MF19134

Cornwall, C. E., Revill, A. T., Hall-Spencer, J. M., Milazzo, M., Raven, J. A., and Hurd, C. L. (2017). Inorganic carbon physiology underpins macroalgal responses to elevated CO₂. *Sci. Rep.* 7, 46297. doi: 10.1038/srep46297

Cornwall, C. E., Revill, A. T., and Hurd, C. L. (2015). High prevalence of diffusive uptake of CO₂ by macroalgae in a temperate subtidal ecosystem. *Photosynth. Res.* 124, 181–190. doi: 10.1007/s11120-015-0114-0

Craig, H. (1957). Isotopic standards for carbon and oxygen and correction factors for mass-spectrometric analysis of carbon dioxide. *Geochimica Cosmochimica Acta* 12, 133–149. doi: 10.1016/0016-7037(57)90024-8

de los Santos, C. B., Egea, L. G., Martins, M., Santos, R., Masqué, P., Peralta, G., et al. (2022). Sedimentary organic carbon and nitrogen sequestration across a vertical gradient on a temperate wetland seascape including salt marshes, seagrass meadows and rhizophytic macroalgal beds. *Ecosystems*. 26, 826–842. doi: 10.1007/s10021-022-00801-5

Diaz-Pulido, G., Cornwall, C., Gartrell, P., Hurd, C., and Tran, D. V. (2016). Strategies of dissolved inorganic carbon use in macroalgae across a gradient of terrestrial influence: implications for the Great Barrier Reef in the context of ocean acidification. *Coral Reefs* 35, 1327–1341. doi: 10.1007/s00338-016-1481-5

Dolliver, J., and O'Connor, N. (2022). Whole system analysis is required to determine the fate of macroalgal carbon: A systematic review. *J. Phycol.* 58, 364–376. doi: 10.1111/jpy.13251

Duarte, C. M., Gattuso, J.-P., Hancke, K., Gundersen, H., Filbee-Dexter, K., Pedersen, M. F., et al. (2022). Global estimates of the extent and production of macroalgal forests. *Global Ecol. Biogeogr.* 31, 1422–1439. doi: 10.1111/geb.13515

Falkowski, P. G., and Raven, J. A. (2013). *Aquatic Photosynthesis*. 2nd ed. (Elsevier, Princeton University Press).

Giordano, M., Beardall, J., and Raven, J. A. (2005). CO₂ CONCENTRATING MECHANISMS IN ALGAE: mechanisms, environmental modulation, and evolution. *Annu. Rev. Plant Biol.* 56, 99–131. doi: 10.1146/annurev.arplant.56.032604.144052

Gordon, L. I., Jennings, J. C., Ross, A. A., and Krest, J. M. (1992). A suggested protocol for continuous flow automated analysis of seawater nutrients in the WOCE hydrographic program and the joint global ocean fluxes study. *Grp. Tech Rpt 92-1 OSU Coll. Oceanography Descr. Chem. Oc.*

Hager, S. W., Atlas, E. L., Gordon, L. I., Mantyla, A. W., and Park, P. K. (1972). A comparison at sea of manual and autoanalyzer analyses of phosphate, nitrate, and silicate. *Limnol. Oceanogr.* 17, 931–937. doi: 10.4319/lo.1972.17.6.0931

Hama, T., Miyazaki, T., Ogawa, Y., Iwakuma, T., Takahashi, M., Otsuki, A., et al. (1983). Measurement of photosynthetic production of a marine phytoplankton population using a stable 13C isotope. *Mar. Biol.* 73, 31–36. doi: 10.1007/BF00396282

Hayes, J. (2004). *An Introduction to Isotopic Calculations* (Woods Hole Oceanographic Institution). doi: 10.1575/1912/27058

Hepburn, C. D., Pritchard, D. W., Cornwall, C. E., McLEOD, R. J., Beardall, J., Raven, J. A., et al. (2011). Diversity of carbon use strategies in a kelp forest community: implications for a high CO₂ ocean. *Global Change Biol.* 17, 2488–2497. doi: 10.1111/j.1365-2486.2011.02411.x

Houlihan, E. P., Espinel-Velasco, N., Cornwall, C. E., Pilditch, C. A., and Lamare, M. D. (2020). Diffusive boundary layers and ocean acidification: implications for sea urchin settlement and growth. *Front. Mar. Sci.* 7. doi: 10.3389/fmars.2020.577562

Hurd, C. L. (2000). Water motion, marine macroalgal physiology, and production. *J. Phycol.* 36, 453–472. doi: 10.1046/j.1529-8817.2000.99139.x

James, R. K., Hepburn, C. D., Pritchard, D., Richards, D. K., and Hurd, C. L. (2022). Water motion and pH jointly impact the availability of dissolved inorganic carbon to macroalgae. *Sci. Rep.* 12, 21947. doi: 10.1038/s41598-022-26517-z

Ji, Y., and Gao, K. (2021). Effects of climate change factors on marine macroalgae: A review. *Adv. Mar. Biol.* (Elsevier) 88, 91–136. doi: 10.1016/bs.amb.2020.11.001

Krause-Jensen, D., Marbà, N., Sanz-Martin, M., Hendriks, I. E., Thyrring, J., Carstensen, J., et al. (2016). Long photoperiods sustain high pH in Arctic kelp forests. *Sci. Adv.* 2, e1501938. doi: 10.1126/sciadv.1501938

Kroopnick, P. M. (1985). The distribution of 13C of Σ CO₂ in the world oceans. *Deep Sea Res. Part A Oceanographic Res. Papers* 32, 57–84. doi: 10.1016/0198-0149(85)90017-2

La Valle, F. F., Jacobs, J. M., Thomas, F. I., and Nelson, C. E. (2023). Nutrient-rich submarine groundwater discharge increases algal carbon uptake in a tropical reef ecosystem. *Front. Mar. Sci.* 10. doi: 10.3389/fmars.2023.1178550

La Valle, F. F., Thomas, F. I., and Nelson, C. E. (2019). Macroalgal biomass, growth rates, and diversity are influenced by submarine groundwater discharge and local hydrodynamics in tropical reefs. *Mar. Ecol. Prog. Ser.* 621, 51–67. doi: 10.3389/meps12992

Littler, M. M., and Arnold, K. E. (1982). Primary productivity of marine macroalgal functional-form groups from southwestern North America. *J. Phycol.* 18, 307–311. doi: 10.1111/j.1529-8817.1982.tb03188.x

Littler, M. M., and Littler, D. S. (1981). Intertidal macrophyte communities from Pacific Baja California and the upper gulf of California: relatively constant vs. environmentally fluctuating systems. *Mar. Ecol. Prog. Ser.* 4, 145–158.

Littler, M. M., and Murray, S. N. (1974). The primary productivity of marine macrophytes from a rocky intertidal community. *Mar. Biol.* 27, 131–135. doi: 10.1007/BF00389065

Lovelock, C. E., Reef, R., Raven, J. A., and Pandolfi, J. M. (2020). Regional variation in δ¹³C of coral reef macroalgae. *Limnol. Oceanogr.* 65, 2291–2302. doi: 10.1002/lo.11453

Maberly, S. C., Raven, J. A., and Johnston, A. M. (1992). Discrimination between 12C and 13C by marine plants. *Oecologia* 91, 481–492. doi: 10.1007/BF00650320

Mann, K. H. (1973). Seaweeds: their productivity and strategy for growth | *Science*. *Science* 182, 975 — 981. doi: 10.1126/science.182.4116.975

Mateo, M. A., Renom, P., Hemminga, M. A., and Peele, J. (2001). Measurement of seagrass production using the 13C stable isotope compared with classical O₂ and 14C methods. *Mar. Ecol. Prog. Ser.* 223, 157–165. doi: 10.3354/meps223157

Miller, H. L., and Dunton, K. H. (2007). Stable isotope (13C) and O₂ micro-optode alternatives for measuring photosynthesis in seaweeds. *Mar. Ecol. Prog. Ser.* 329, 85–97. doi: 10.3354/meps329085

Murray, S. N., and Bray, R. N. (1993). Benthic macrophytes. Ecology of the Southern California Bight: a synthesis and interpretation 304–368.

Pace, M. L., and Lovett, G. M. (2013). “Chapter 2 - primary production: the foundation of ecosystems,” in *Fundamentals of Ecosystem Science*. Eds. K. C. Weathers, D. L. Strayer and G. E. Likens (Academic Press), 27–51. doi: 10.1016/B978-0-08-091680-4.00002-0

Pessarrodona, A., Assis, J., Filbee-Dexter, K., Burrows, M. T., Gattuso, J.-P., Duarte, C. M., et al. (2022). Global seaweed productivity. *Sci. Adv.* 8. doi: 10.1126/sciadv.abn2465

Peterson, B. J. (1980). Aquatic primary productivity and the 14C-CO₂ method: A history of the productivity problem. *Annu. Rev. Ecol. Evol. Syst.* 11, 359–385. doi: 10.1146/annurev.es.11.110180.002043

Pfister, C. A., Altabet, M. A., and Weigel, B. L. (2019). Kelp beds and their local effects on seawater chemistry, productivity, and microbial communities. *Ecology* 100, e02798. doi: 10.1002/ecy.2798

Queirós, A. M., Tait, K., Clark, J. R., Bedington, M., Pascoe, C., Torres, R., et al. (2023). Identifying and protecting macroalgal detritus sinks toward climate change mitigation. *Ecol. Appl.* 33, e2798. doi: 10.1002/eap.2798

Rautenberger, R., Fernández, P. A., Strittmatter, M., Heesch, S., Cornwall, C. E., Hurd, C. L., et al. (2015). Saturating light and not increased carbon dioxide under ocean acidification drives photosynthesis and growth in *Ulva rigida* (Chlorophyta). *Ecol. Evol.* 5, 874–888. doi: 10.1002/ece3.1382

Raven, J. A., and Hurd, C. L. (2012). Ecophysiology of photosynthesis in macroalgae. *Photosynth. Res.* 113, 105–125. doi: 10.1007/s11120-012-9768-z

Raven, J. A., Johnston, A. M., Kübler, J. E., Korb, R., McInroy, S. G., Handley, L. L., et al. (2002). Mechanistic interpretation of carbon isotope discrimination by marine macroalgae and seagrasses. *Funct. Plant Biol.* 29, 355–378. doi: 10.1071/pp01201

Raven, J., Walker, D., Johnston, A., Handley, L., and Kübler, J. (1995). Implications of 13C natural abundance measurements for photosynthetic performance by marine macrophytes in their natural environment. *Mar. Ecol. Prog. Ser.* 123, 193–205. doi: 10.3354/meps123193

Ruhamak, B. A., Hamdani, H., Rostini, I., and Sahidin, A. (2019). *Macroalgae Association with Invertebrate Biota in Madasari Coast* Vol. 7 (West Java, Indonesia).

Ryznar, E. R., Fong, P., and Fong, C. R. (2021). When form does not predict function: Empirical evidence violates functional form hypotheses for marine macroalgae. *J. Ecol.* 109, 833–846. doi: 10.1111/1365-2745.13509

Spector, M., and Edwards, M. S. (2020). Species-specific biomass drives macroalgal benthic primary production on temperate rocky reefs. *Algae* 35, 237–252. doi: 10.4490/algae.2020.35.8.19

Stewart, and Carpenter, (2003). The effects of morphology and water flow on photosynthesis of marine macroalgae. *Ecology* 84, 2999–3012. doi: 10.1890/02-0092

Strickland, J. D. (1960). Measuring the production of marine phytoplankton. *Fish. Res. Bd. Canada Bull.* 122, 172.

Tait, L. W., and Schiel, D. R. (2018). Ecophysiology of layered macroalgal assemblages: importance of subcanopy species biodiversity in buffering primary production. *Front. Mar. Sci.* 5. doi: 10.3389/fmars.2018.00444

Teichberg, M., Fox, S. E., Aguilera, C., Olsen, Y. S., and Valiela, I. (2008). Macroalgal responses to experimental nutrient enrichment in shallow coastal waters: growth, internal nutrient pools, and isotopic signatures. *Mar. Ecol. Prog. Ser.* 368, 117–126. doi: 10.3354/meps07564

Thomas, F. I. M., and Cornelisen, C. D. (2003). Ammonium uptake by seagrass communities: effects of oscillatory versus unidirectional flow. *Mar. Ecol. Prog. Ser.* 247, 51–57. doi: 10.3354/meps247051

Torres, M. E., Mix, A. C., and Rugh, W. D. (2005). Precise δ¹³C analysis of dissolved inorganic carbon in natural waters using automated headspace sampling and continuous-flow mass spectrometry. *Limnol. Oceanogr.: Methods* 3, 349–360. doi: 10.4319/lom.2005.3.349

Tsubaki, S., Nishimura, H., Imai, T., Onda, A., and Hiraoka, M. (2020). Probing rapid carbon fixation in fast-growing seaweed *Ulva meridionalis* using stable isotope 13C-labelling. *Sci. Rep.* 10, 20399. doi: 10.1038/s41598-020-77237-1

van der Loos, L. M., Schmid, M., Leal, P. P., McGraw, C. M., Britton, D., Revill, A. T., et al. (2018). Responses of macroalgae to CO₂ enrichment cannot be inferred solely from their inorganic carbon uptake strategy. *Ecol. Evol.* 9, 125–140. doi: 10.1002/ece3.4679

Velázquez-Ochoa, R., Ochoa-Izaguirre, M. J., and Soto-Jiménez, M. F. (2022). An analysis of the variability in $\delta^{13}\text{C}$ in macroalgae from the Gulf of California: indicative of carbon concentration mechanisms and isotope discrimination during carbon assimilation. *Biogeosciences* 19, 1–27. doi: 10.5194/bg-19-1-2022

Williamson, C. J., Perkins, R., Voller, M., Yallop, M. L., and Brodie, J. (2017). The regulation of coralline algal physiology, an *in situ* study of *Corallina officinalis* (Corallinales, Rhodophyta). *Biogeosciences* 14, 4485–4498. doi: 10.5194/bg-14-4485-2017

Yacobi, Y. Z., Perel, N., Barkan, E., and Luz, B. (2007). Unexpected underestimation of primary productivity by ^{18}O and ^{14}C methods in a lake: Implications for slow diffusion of isotope tracers in and out of cells. *Limnol. Oceanogr.* 52, 329–337. doi: 10.4319/lo.2007.52.1.0329

Young, E. B., and Beardall, J. (2005). Modulation of photosynthesis and inorganic carbon acquisition in a marine microalga by nitrogen, iron, and light availability. *Can. J. Bot.* 83, 917–928. doi: 10.1139/b05-081

Zweng, R. C., Koch, M. S., and Bowes, G. (2018). The role of irradiance and C-use strategies in tropical macroalgae photosynthetic response to ocean acidification. *Sci. Rep.* 8, 9479. doi: 10.1038/s41598-018-27333-0